Spatiotemporal structure of the lidar return component due to multiple scattering

V.V. Belov and A.B. Serebrennikov

Institute of Atmospheric Optics,
Siberian Branch of the Russian Academy of Sciences, Tomsk

Received December 29, 1999

The results of Monte Carlo simulation of the spatiotemporal structure of the lidar return component due to multiple scattering are analyzed for the case of monostatic sensing geometry. It is shown that the instantaneous brightness body of multiply scattered radiation may have large volume, not coinciding with the region where the single-scattering signal comes from. The main factor influencing the spatial and brightness characteristics of this volume source are determined.

Introduction

One of the main limitations of lidar systems, as a means for diagnostic of the optical, microphysical, and other characteristics of scattering media is that the theory of solution of inverse laser sensing problems[1] is based on solution of the radiative transfer equation in the single scattering approximation. For this reason, in most cases lidar methods are only applicable to studies of optically thin scattering media and they may become inefficient in interpreting lidar returns from the media that are far from the lidar system (for instance in sensing the near-ground layer from space[2]).

In other words, the lidar sensing instruments are only applicable for diagnostics of thin, closest to the lidar receiver, boundary layer of a turbid media, characterized by the optical depths $\tau < 2$. This is true because the relative contribution of multiply scattered radiation to the return signal increases as the laser beam penetrates deeper and deeper into an optically dense medium, eventually becoming comparable with, or even larger than, the signal (by which we usually mean the radiation singly scattered toward a receiver and falling within its field of view (FOV)).

For a wider use of lidar sensing techniques in diagnostics of optically dense scattering media, it is necessary to develop a new theory of solving the inverse problems[3] of laser sensing (in which total recorded signal would have been the useful one). Also helpful could be creation of reliable methods of extracting the lidar return component due to single scattering from the total signal for its subsequent interpretation by traditional methods. Progress in both of these research areas of development of the theory of laser sensing of scattering media will make it possible to address a wider scope of problems in remote diagnostics of dense scattering media with $\tau \geq 2$ (fogs, clouds, smoke plumes in the atmosphere, polydisperse systems in biological substances, etc.).

In this paper, we present the results of analysis of spatiotemporal structure of the lidar return component due to multiple scattering in sensing of optically dense scattering media. This work was initiated by scientific seminars at the Institute of Atmospheric Optics in 1999 and devoted to the problems of multiple scattering, new methods of sensing of optically dense media, and interpretation of laser return signals in sensing geometry with variable-FOV receivers.

Problem formulation

In the theory of inverse problems of laser sensing, which is based on the lidar equation written in the single scattering approximation,[1] the term "depth of beam penetration" into the scattering medium is quite common. This notion is frequently associated with the spatial region in the neighborhood of the point M located at a distance r from the lidar receiver at its optical axis; at this point, the characteristics of the medium are retrieved from a lidar return $h(t)$ at the time $t = 2r/c$ (where c is the speed of light; and for simplicity, monostatic or coaxial viewing geometry is assumed).

The pulsed response of the sensing channel,[4] for the case of sensing the spatially bounded scattering layers with the thickness L, has the duration $T > 2L/c$ (if time is counted from the moment $t_0 = 2r_0/c$, where r_0 is the distance between the source and the layer boundary closest to it). In this case, the question on spatially referencing the retrieved results for the moments in time $t > 2L/c$ remains open. Let us turn to Fig. 1, which presents the results of statistical simulation of the pulsed response $h(t)$ of a monostatic sensing channel for the case of sensing a remote cloud layer, in which the extinction coefficient increases with the increasing depth into the cloud. Arrow shows time $t > 2L/c$, corresponding to the fictitious depths of beam penetration to the cloud. This follows from the model assuming no cloud particles and scattering interactions at $r > L$, and, hence, no photons coming to the receiver from this region of space.

0235-6880/00/08 671-06 $02.00

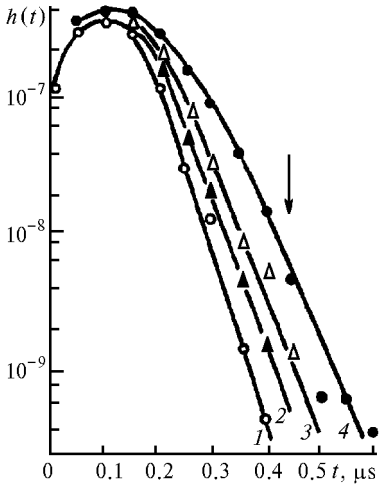

Fig. 1. Family of pulsed responses of inhomogeneous channel of cloud sensing. Calculations were made for the receiver's FOVs of 10′ (curve *1*), 30′ (curve *2*), 1° (curve *3*), and 3° (curve *4*) and for $\tau = 4$.

Suppose that there is some procedure or operator E by which, using any rules, the value of $h(t)$ at a time t is converted to the optical characteristic K in a certain region **R** of the medium sensed

$$E[h(t)] = K(\mathbf{R}).$$

The region **R** is uniquely related, by the lidar equation, to time t of recording the return signal and, once the beam divergence and width have been neglected, it degenerates to the point at $r = ct/2$. If this procedure of $h(t)$ interpretation is applied to situation depicted in Fig. 1 (for $t > 2L/c$), then one obviously obtains certain nonzero values of the optical characteristics instead of zero ones. The signal $h(t)$ at $t > 2L/c$ is formed by photons coming to the detector from the medium in which they were multiply scattered and traversed the path $l > 2L$.

Obviously, the component due to multiple scattering is also present in the return signal at the measurement times $t < 2L/c$. Moreover, its level may exceed that of the single scattering component,[4] which rapidly (proportionally to $\exp(-\tau)/r^2$) decays with time that reduces the applicability of the lidar equation to diagnostics of such media. Indeed, even if the component due to multiple scattering is eliminated from lidar return by any (such as polarization-sensitive) technique, the residual signal will not exceed the instrumental noise level. This explains why new methods of sensing (such as those based on the variable-FOV detectors[5]) and interpretation of data of remote laser sensing of optically dense scattering media are now being actively developed.

Of course, multiply scattered radiation bears information on the medium it comes from, but before extracting it, it is necessary to identify the mechanisms of formation of this component of a signal from the medium. This problem was addressed in many theoretical and experimental studies, the most comprehensive, in our opinion, being the studies discussed in Refs. 4 and 6. Well studied are the issues concerning the temporal structure of the background due to multiple scattering in the lidar returns. In particular, the influence of different orders of multiple scattering on this component of return signals is estimated,[6] and time response of this component to variations of the optical characteristics of the medium and parameters of viewing geometry[4] is investigated.

It is unclear, however, what is the spatiotemporal structure of the lidar return component due to multiple scattering (Fig. 2), i.e., which regions of the medium contribute to this component at each particular moment in time, and how these regions are defined by the optical parameters and sensing geometry. In this paper we give answers to these questions in the context of the problem formulated as follows.

Let a monochromatic point source of radiation at the wavelength λ with the beam divergence $2\nu_0$ is located at the origin O of a Cartesian coordinate system (Fig. 3). Let also the beam propagates along the direction parallel to Oy-axis. We assume a coaxial monostatic sensing geometry. The detector FOV angle is $2\nu_1$. The scattering medium is stratified and involves plane-parallel layers with the boundaries parallel to the xOz plane; it is infinite in the directions $\mathbf{n} \perp Oy$, and is bounded by the planes $y = 0$ and $y = L$.

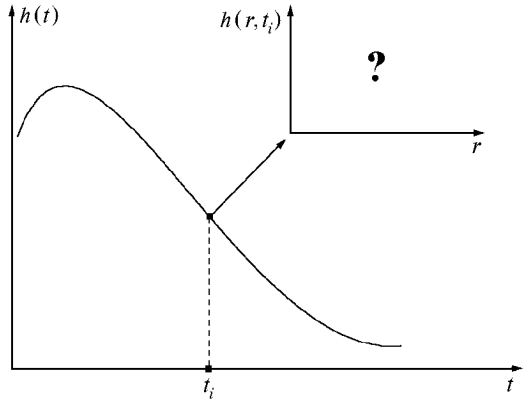

Fig. 2. Illustrative formulation of the problem on determining the spatiotemporal structure of lidar return.

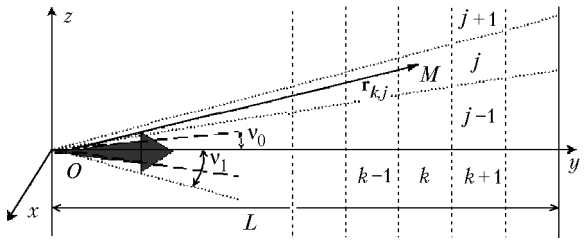

Fig. 3. Viewing geometry used in the numerical experiments.

The optical properties of the medium are determined by the extinction $\beta_{ext}(y)$, scattering $\beta_{sct}(y)$, and absorption $\beta_{ab}(y)$ coefficients and by the scattering phase function $g(\mu)$ (where μ is the cosine of scattering

angle) corresponding to a cloud or aerosol spherical polydispersions. The source is assumed to emit a $\delta(t)$ pulses. We aim at determining the influence of the optical and geometrical parameters of sensing on the pulsed responses $h(t)$, $h_1(t)$, $h_m(t)$, $h(t, \mathbf{r})$, $h_m(t, \mathbf{r})$, and $h_1(t, \mathbf{r})$. Here, $h = h_1 + h_m$, $\mathbf{r}$ is the position vector of a point in the scattering medium, and subscripts 1 and m denote quantities calculated taking first and all but first scattering orders into account.

Method and models of medium used in the study

The Monte Carlo estimates on straight lines are obtained using the method of local estimates,[7] which in our case is expressed by the following formula:

$$l_{i,j,k} \approx \frac{\omega_{k,j}\, g(\mu_{k,j}) \exp(-\tau_{k,j})}{2\pi r_{k,j}^2} \Delta_i ,$$

where k is the number of the layer where a scattering event occurred; j is the number of the narrowest detector FOV containing the point $\mathbf{r}_{k,j}$ (see Fig. 3); Δ_i is the indicator of time interval $(t_i - t_{i-1})$ representing the photon "lifetime", that is the period from photon emission along the trajectory of travel, that passes through the point $\mathbf{r}_{k,j}$, and ends at the detector; and $\omega_{k,j}$ is the photon statistical weight to account for photon absorption during travel.

During numerical experiments we controlled the simulation error. The rms error in our calculations did not exceed 20%. Where not burdensome, this error is shown in Figs. 7–9 by the error bars.

The directional light scattering was modeled using scattering phase functions of the urban aerosol and fogs of two types (advective and radiative) at the wavelength $\lambda = 0.86$ μm.[8] In the numerical experiments it was assumed that the geometrical thickness L of the medium is fixed to be 1000 m. The optical depth was varied in the range $2 \le \tau \le 8$ by changing the extinction coefficient in each layer, while keeping the single scattering albedo constant $\chi = \beta_{sct}(y)/\beta_{ext}(y) = \text{const}$. This model of optical properties of the medium can be used first for determining the dependence of the studied characteristics of the medium on its optical depth and/or asymmetry (forward peakedness) of the scattering phase function. To see how inhomogeneity of the optical properties of the medium influences the component due to multiple scattering, we specified a uniform profile of extinction coefficient, i.e., $\beta_{ext}(y) = \text{const}$ (curve *1*) as well as "increasing" one (Fig. 4, curve *2*).

The dependence of the component due to multiple scattering on absorption is easier to predict because a decrease in the single scattering albedo causes a suppression of multiple scattering process and a monotonic decrease of its contribution to lidar returns. Therefore, the single scattering albedo was not varied throughout the numerical simulation.

The shape of the scattering phase function will be characterized by the coefficients

$$\gamma = \int_0^1 g(\mu)\, d\mu \Big/ \int_{-1}^1 g(\mu)\, d\mu; \quad \xi = g(1)/g(-1).$$

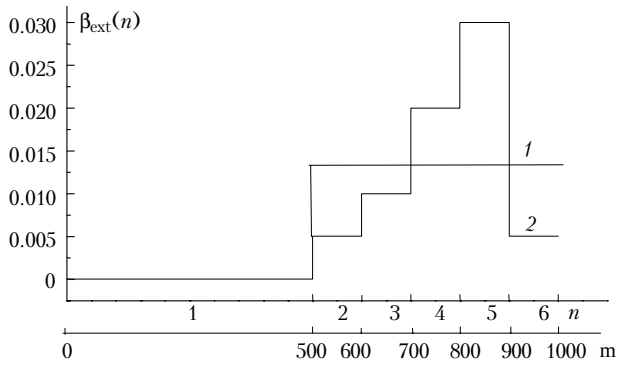

Fig. 4. Profiles of the extinction coefficient along the optical axis of a laser beam, which were used in calculations (here n is the layer number in the plane parallel model of a stratified scattering medium).

For the $g(\mu)$ models chosen here, the coefficient γ ranges from 0.7995 (urban aerosol) to 0.984 (radiative fog), while the coefficient ξ varies from 723 (advective fog) to 27200 (radiative fog).

In the calculations, the laser beam divergence was taken to be constant ($\nu_0 = 3'$), while the detector FOV angle ranged from 3 minutes of arc to 5°.

Results

Before proceeding to analysis of statistical simulation results, two remarks are in order. For the viewing geometry considered here (see Fig. 3), the single- and multiple scattering effects on the pulsed response $h(t)$ of the sensing channel are most easily compared for times t of returns from the region near far boundary of the medium. This is because the relative level of the component due to multiple scattering, in this case, (see, e.g., Ref. 4) is higher than that at earlier times of signal recording. The general features of forming the brightness body of multiple scattering remain the same at each moment in time $t < 2L/c$, but at $t \approx 2L/c$ they are, probably, manifest themselves most obviously. Therefore, we will illustrate some results of numerical experiments obtained in the interval $t_i = [2L/c - \varepsilon, 2L/c]$, where $\varepsilon > 0$.

For development of laser sensing systems with a variable receiver's FOV, it is necessary to know how the component of a recorded signal due to multiple scattering depends on ν_1. This dependence is presented in Figs. 5 and 6. Figure 5 shows functions $F(t_i) = h_m(t_i)/h(t_i)$ for aerosol model of the scattering medium with the increasing profile of $\beta_{sct}(y)$, for a set of ν_1 values and optical depths $\tau = 2$, 4, and 8. For all τ values, there is a tendency in the ratio $F(t_i)$ toward

saturation on a constant level. As τ increases, the leveling-off occurs for smaller FOVs.

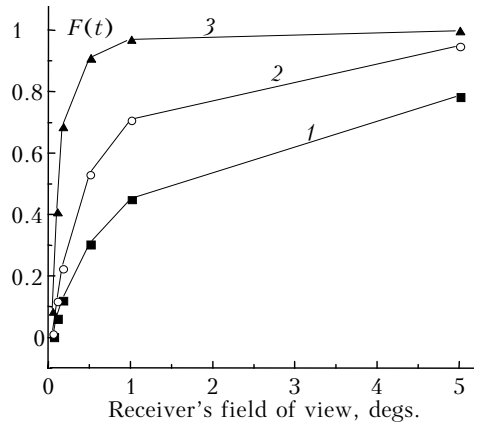

Fig. 5. Influence of the optical depth of the medium on the dependence of the ratio $F(t_i) = h_m(t_i)/h(t_i)$ on the receiver's FOV: $\tau = 2$ (curve *1*); 4 (curve *2*); and 8 (curve *3*). Aerosol characteristics are for $\lambda = 0.86$ μm, $\gamma = 0.7995$, and $\xi = 1637$.

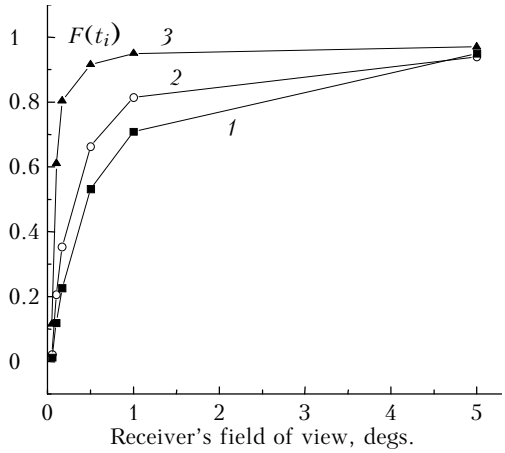

Fig. 6. The dependence of multiple-scattering contribution to pulsed response $h(t_i)$ on the receiver's FOV for different models of scattering media: aerosol with $\gamma = 0.7995$ and $\xi = 1637$ (curve *1*); fog with $\gamma = 0.945$ and $\xi = 723$ (curve *2*); and fog with $\gamma = 0.989$, $\xi = 27200$, $\tau = 2$ at $\lambda = 0.86$ μm (curve *3*).

This is not surprising considering that in the calculations, the increase of the optical depth of the medium was modeled by increasing the concentration of aerosol particles, while keeping the geometrical thickness of the medium constant. In this case, the larger τ, the shorter the photon mean free path, and, hence, the smaller the angular dimensions of the beam, smeared in the medium and visible from the center of receiver's aperture.

The visible beam width saturates because, as the beam penetrates into the medium and multiple scattering effect intensifies, there also occurs an increase of the optical depth of the region that screens the receiver from laser radiation. It is expected, therefore, that, with the increasing receiver's FOV and, hence, with the growth of the volume contributing to this process, the number of multiply scattered photons coming back to the receiver will increase only to a certain level, until the amount of scattered energy increase is compensated for by its attenuation in the volume. As a result, the increasing FOV in excess of some fixed value, probably, will not lead to a significant increase of $h(t_i)$.

The influence of the shape of the scattering phase function on $F(t_i)$ is illustrated in Fig. 6, where $F(t_i)$ is plotted as a function of the receiver's FOV for the model media such as aerosol and fog (advective and radiative) at $\tau = 4$. Again we see the tendency in the contribution due to multiple scattering to $h(t_i)$ to saturate at a constant level with the increasing FOV. This can be explained following the same argument as in discussion of Fig. 5. The stronger the forward peakedness of the scattering phase function, the faster the ratio $h_m(t_i)/h(t_i)$ saturates. This is because the stronger the forward peakedness of the scattering phase function, the faster the beam broadening occurs at the beam penetration into the medium. In the limiting case when the scattering phase function $g(\boldsymbol{\omega}, \boldsymbol{\omega}') = \delta(\boldsymbol{\omega} \pm \boldsymbol{\omega}')$, where $\boldsymbol{\omega}$ and $\boldsymbol{\omega}'$ are the directions of photon travel before and after a scattering event, the beam preserves its shape and, starting from some $\nu_1 \geq \nu_0$, $h(t_i)$ does not depend on the receiver's FOV.

Let us now turn to the structure of instantaneous brightness body of scattered radiation, i.e., to the spatial and energy characteristics of the region of the medium which, in the multiple-scattering process, becomes the source of secondary (multiply scattered) radiation flux, recorded during time interval $t_i = [2L/c - \varepsilon, \ 2L/c]$. The shape and brightness distribution of this source is well quantified by the ratio $G(n, t_i) = h_m(n, t_i)/h(t_i)$, where n is the number of the layer of the medium (counted from the layer closest to the source), from which the photons come to the receiver with a given aperture at the time instant t_i. It characterizes the relative contributions of different parts of the medium to the pulsed response $h(t_i)$. We note that $h_m(n, t_i)$ has the meaning of the power of multiply scattered radiation coming to the receiver from the region defined by the receiver's FOV cone angle and bounding planes of the nth layer of the medium.

Figures 7*a* and *b* present the functions $G(n, t_i)$ plotted for the aerosol model of the medium with the increasing profile $\beta_{ext}(y)$. When optical depth is relatively small ($\tau = 4$, see Fig. 7*a*), the return signal due to multiple scattering comes largely from the region adjacent to the region where the single scattering signal $h_1(t_i)$ comes from. The closer the layer to the source region, the less its contribution to the $h(t_i)$ signal. The influence of angular aperture of the receiver on $G(n, t_i)$ is as follows: its increase leads to (1) a growth of contribution to $h(t_i)$ from the regions closest to the receiver, and (2) to a decrease of the influence of the region closest to region where the reflected pulse $h_1(t_i)$ comes from; nonetheless the second factor remains dominant given detector FOVs 0.5 and 1°.

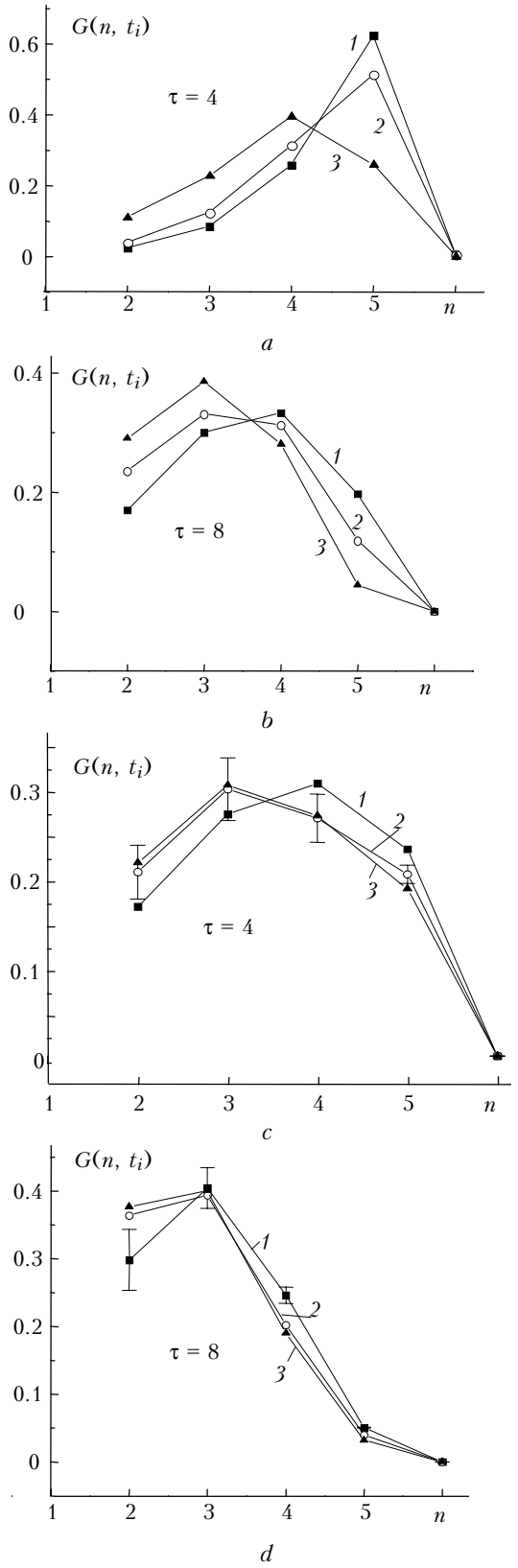

Fig. 7. Spatial structure function $G(n, t_i)$ of multiply scattered component at the time t_i for (*a*, *b*) aerosol layer with $\gamma = 0.7995$ and $\xi = 1637$ at $\lambda = 0.86$ μm; and (*c*, *d*) fog layer with $\gamma = 0.98895$ and $\xi = 27200$. The detector FOV is 0.5° (curve *1*), 1° (curve *2*), and 5° (curve *3*).

As the optical depth of the medium increases to $\tau = 8$ (see Fig. 7*b*), the pattern of signal distribution drastically changes. As the receiver's FOV increases, the contribution of the first layers becomes dominant.

Changes in the brightness body $G(n, t_i)$ in response to an increase in the forward peak of the scattering phase function are illustrated in Figs. 7*c* and *d*. These data differ from those discussed above (see Figs. 7*a* and *b*) only in that they are calculated for a radiative fog. From data in Figs. 7*c* and *d* it follows that as the scattering phase function becomes more asymmetric in the forward direction, the influence of the receiver's FOV on $G(n, t_i)$ increases, and contribution from the "middle" layers of the medium far from the receiver increases as well as from the region where the single scattering signal comes from. This conclusion is further confirmed by Fig. 8, which gives $G(n, t_i)$ for the media and observation conditions different only in the scattering phase function.

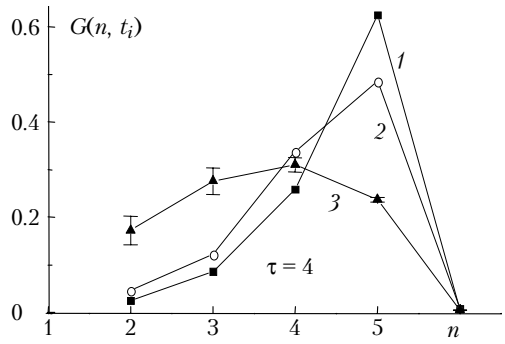

Fig. 8. Brightness body of the multiply scattered radiation recorded by a detector at the time t_i (see Fig. 2) for different models of the medium (the same as in Fig. 6).

The influence of the profile $\beta_{sct}(y)$ on the shape of the function $G(n, t_i)$ can be assessed using data presented in Fig. 9, where the families of $G(n, t_i)$ curves are plotted for the models of uniform and increasing $\beta_{sct}(y)$ function. For an aerosol medium with a given density and for a particular receiver's FOV, the shape of the instantaneous brightness body little depends on the extinction coefficient profile $\beta_{sct}(y)$ (Fig. 9*a*). On the other hand, simulation results for denser media and wider detector FOVs suggest that an increase in either of these parameters leads to a larger difference in signal layering between homogeneous and inhomogeneous media. As seen from Fig. 9*b*, when scattering phase function has strong forward peakedness, even at the parameters as small as $\tau = 4$ and $\nu_1 = 0.5°$, the functions $G(n, t_i)$ for different models of $\beta_{sct}(y)$ is substantially different. Thus, the shape of the angular scattering pattern can also substantially influence the difference in distribution of pulsed response between homogeneous and inhomogeneous media.

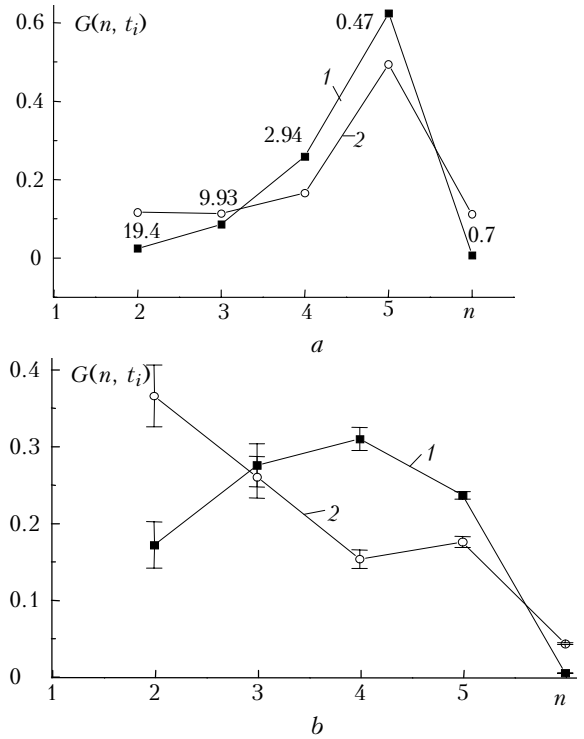

Fig. 9. Comparison of the functions $G(n, t_i)$, obtained for aerosol (*a*) and radiative fog (*b*) models of scattering medium with uniform and increasing profiles $\beta_{ext}(y)$. Numbers near curves indicate standard deviation in percent. Calculations were made for $\tau = 4$ and $\nu_1 = 0.5°$ assuming inhomogeneous (curve *1*) and homogeneous (curve *2*) medium.

Conclusions

From analysis of results obtained by numerical Monte Carlo method, the following preliminary (and valid within the considered ranges of sensing parameter values) conclusions can be drawn.

1. When the receiver's FOV exceeds the laser beam divergence, the lidar return from a scattering medium with optical depth $\tau > 1$ can be determined by the extended regions nearer to the receiver than the region where single scattering component comes from.

2. This region constitutes a volume source of multiply scattered radiation (recorded at the same time), which is characterized by the brightness variations both across the receiver's FOV and along the direction of laser beam propagation.

3. Brightness of particular parts of this region significantly depends on the optical depth of the medium and forward peakedness of the scattering phase function. For narrow receiver's FOV, the maximum contribution from multiple scattering to a lidar return comes from rather a thin region adjacent to the region where single-scattering signal comes from. With increasing optical depth of the medium, the receiver's FOV, and asymmetry of the scattering phase function, the spatial region making up most of the multiple scattering signal grows in size and shifts toward the source.

4. The inhomogeneity of the scattering properties of a stratified medium, which depend, within some ranges of ν_1 and τ values, on the shape of the scattering phase function, does not lead to serious change of the instantaneous brightness body of the multiply scattered radiation in the receiver's FOV.

Summarizing the above-said, one can state that for construction of new methods of interpretation of remote sensing data on optically dense media, that treat the component due to multiple scattering as a useful signal, it is necessary to take the spatiotemporal structure of this component into account. This would make it possible to relate correctly the time of measurement of lidar signal and the characteristics of spatial region under study and, thereby, to determine the physical meaning of the latter adequately.

Acknowledgments

Authors thank the participants of seminars, held at IAO SB RAS and devoted to problems in multiple scattering and new methods of sensing optically dense scattering media, for the fruitful discussion of the results presented here.

References

1. V.E. Zuev and I.E. Naats, *Inverse Problems in Atmospheric Optics* (Gidrometeoizdat, Leningrad, 1990), 286 pp.
2. C.V. Samoilova, Yu.S. Balin, and M.M. Krekova, Atmos. Oceanic Opt. **11**, No. 1, 50–54 (1998).
3. E.P. Zege, I.L. Katsev, and I.N. Polonskii, Izv. Akad. Nauk SSSR, Ser. Fiz. Atmos. Okeana **34**, No. 1, 45–50 (1998).
4. V.E. Zuev, V.V. Belov, and V.V. Veretennikov, *Theory of Systems in Optics of Disperse Media* (Publishing House of SB RAS, Tomsk, 1997), 402 pp.
5. V.V. Veretennikov, Proc. SPIE **3983**, *Sixth International Symposium on Atmospheric and Ocean Optics*, 364–371 (1999).
6. M.M. Krekova, Atmos. Oceanic Opt. **12**, No. 4, 362–367 (1999).
7. G.I. Marchuk, ed., *Monte Carlo Method in Atmospheric Optics*, (Nauka, Novosibirsk, 1976), 216 pp.
8. F.X Kneizys et al., *User Guide to LOWTRAN–7*, AFGL–TR–86–01777. ERP N 1010 / Nanscom AFB, MA01731.